Pretreatment Tissue TCR Repertoire Evenness Is Associated with Complete Pathologic Response in Patients with NSCLC Receiving Neoadjuvant Chemoimmunotherapy

Marta Casarrubios[1], Alberto Cruz-Bermúdez[1], Ernest Nadal[2], Amelia Insa[3], María del Rosario García Campelo[4], Martín Lázaro[5], Manuel Dómine[6], Margarita Majem[7], Delvys Rodríguez-Abreu[8], Alex Martínez-Martí[9], Javier de Castro-Carpeño[10], Manuel Cobo[11], Guillermo López-Vivanco[12], Edel Del Barco[13], Reyes Bernabé Caro[14], Nuria Viñolas[15], Isidoro Barneto Aranda[16], Santiago Viteri[17], Bartomeu Massuti[18], Miguel Barquín[1], Raquel Laza-Briviesca[1], Belén Sierra-Rodero[1], Edwin R. Parra[19], Beatriz Sanchez-Espiridion[19], Pedro Rocha[19], Humam Kadara[19], Ignacio I. Wistuba[19], Atocha Romero[1], Virginia Calvo[1], and Mariano Provencio[1]

ABSTRACT

Purpose: Characterization of the T-cell receptor (TCR) repertoire may be a promising source for predictive biomarkers of pathologic response to immunotherapy in locally advanced non–small cell lung cancer (NSCLC).

Experimental Design: In this study, next-generation TCR sequencing was performed in peripheral blood and tissue samples of 40 patients with NSCLC, before and after neoadjuvant chemoimmunotherapy (NADIM clinical trial, NCT03081689), considering their complete pathologic response (CPR) or non-CPR. Beyond TCR metrics, tissue clones were ranked by their frequency and spatiotemporal evolution of top 1% clones was determined.

Results: We have found a positive association between an uneven TCR repertoire in tissue samples at diagnosis and CPR at surgery. Moreover, TCR most frequently ranked clones (top 1%) present in diagnostic biopsies occupied greater frequency in the total clonal

space of CPR patients, achieving an AUC ROC to identify CPR patients of 0.967 (95% confidence interval, 0.897–1.000; $P = 0.001$), and improving the results of PD-L1 tumor proportion score (TPS; AUC $= 0.767$; $P = 0.026$) or tumor mutational burden (TMB; AUC $= 0.550$; $P = 0.687$). Furthermore, tumors with high pretreatment top 1% clonal space showed similar immune cell populations but a higher immune reactive gene expression profile. Finally, the selective expansion of pretreatment tissue top 1% clones in peripheral blood of CPR patients suggests also a peripheral immunosurveillance, which could explain the high survival rate of these patients.

Conclusions: We have identified two parameters derived from TCR repertoire analysis that could outperform PD-L1 TPS and TMB as predictive biomarkers of CPR after neoadjuvant chemoimmunotherapy, and unraveled possible mechanisms of CPR involving enhanced tumor immunogenicity and peripheral immunosurveillance.

Introduction

Lung cancer is one of the main leading causes of death by cancer worldwide. Approximately 85% of cases are non–small cell lung cancer (NSCLC), of which one third are diagnosed at locally advanced or stage III disease. Stage III NSCLC is a heterogeneous

disease that includes patients with potentially resectable tumors that could theoretically be cured.

Recently, in NADIM trial (NCT03081689; ref. 1), we have shown that patients treated with neoadjuvant chemoimmunotherapy achieved a progression-free survival (PFS) and overall survival (OS) rates at 2 years of 77% and 90%, respectively, whereas 63% of patients

[1]Servicio de Oncología Médica, Instituto de Investigación Sanitaria Puerta de Hierro-Segovia de Arana (IDIPHISA), Hospital Universitario Puerta de Hierro-Majadahonda, Madrid, Spain. [2]Institut Català d'Oncologia, L'Hospitalet de Llobregat, L'Hospitalet de Llobregat, Barcelona, Spain. [3]Fundación INCLIVA, Hospital Clínico Universitario de Valencia, Valencia, Spain. [4]Hospital Universitario A Coruña, A Coruña, Spain. [5]Hospital Universitario de Vigo, Pontevedra, Spain. [6]Hospital Universitario Fundación Jiménez Díaz, Madrid, Spain. [7]Hospital de la Santa Creu i Sant Pau, Barcelona, Spain. [8]Hospital Insular de Gran Canaria, Las Palmas, Spain. [9]Hospital Universitario e Instituto de Oncología Vall d'Hebron (VHIO), Barcelona, Spain. [10]Hospital Universitario La Paz, Madrid, Spain. [11]Hospital Universitario Regional de Málaga, Málaga, Spain. [12]Hospital Universitario Cruces, Barakaldo, Spain. [13]Hospital Universitario de Salamanca, Salamanca, Spain. [14]Hospital Universitario Virgen del Rocio, Sevilla, Spain. [15]Hospital Clínic, Barcelona, Spain. [16]Hospital Universitario Reina Sofia, Córdoba, Spain. [17]Instituto Oncológico Dr. Rosell. Hospital Universitario Quiron Dexeus, Grupo QuironSalud, Barcelona, Spain. [18]Hospital General de Alicante, Alicante, Spain. [19]Department of Translational Molecular Pathology, The University of Texas MD Anderson Cancer Center, Houston, Texas.

Translational Relevance

The advance of chemoimmunotherapy in locally advanced stages of lung cancer has positioned complete pathologic responses (CPR) as a new relevant clinical entity, with implications for both the differential biology behind these responses and their possible use as an endpoint for assessing therapy efficacy. In this exploratory analysis of the NADIM trial, two biomarkers [top 1% clonal space and T-cell receptor (TCR) evenness], associated with T-cell repertoire imbalance, outperformed the established biomarkers PD-L1 and TMB, regarding CPR prediction after chemoimmunotherapy. In addition, some mechanistic insights are revealed, which imply a higher immunogenicity of tumors with high top 1% clonal space, as well as the presence of a distinctive peripheral immunosurveillance of pretreatment tissue top 1% clones, in patients achieving CPR. Finally, although these findings have potential clinical impact and are hypothesis generating, they are exploratory and need to be confirmed in additional, larger cohorts.

achieve a complete pathologic response (CPR). In addition, the PFS rate in patients with CPR was higher than in non-CPR patients. Although these are encouraging results, with most patients maintaining no evidence of disease status after surgery, some of them do not achieve complete responses and relapse or eventually die. Similar results from the phase III Checkmate 816 trial reinforce the superiority of chemoimmunotherapy compared with chemotherapy alone in the rate of CPR (2). Thus, the identification of biomarkers of CPR to chemoimmunotherapy induction is therefore a priority in the future scenario of resectable NSCLC.

In the context of immunotherapy, both the determination of PD-L1 and tumor mutational burden (TMB) have been carried out to predict which patients are more likely to respond to treatment (3, 4). However, the results are not consistent (5–7) and their value in the context of neoadjuvant chemoimmunotherapy is limited (1, 2). Thus, it is necessary to explore other biomarkers capable of predicting which patients will benefit most from this treatment (8, 9).

The mechanism by which the adaptive immune system responds to immunotherapy and recognizes tumor antigens relies mainly on the highly polymorphic T-cell receptors (TCR) present in an individual. That is why the characterization of the TCR repertoire in terms of clones, diversity, and antigen specificity by sequencing the CDR3 hypervariable region, seems to be a promising approach (10, 11). Other authors have previously reported that parameters extracted from the TCR repertoire were associated with response to immunotherapy in different patients with cancer (12–15) and in particularly, NSCLC (16–18). However, it has not been demonstrated its predictive value in pathologic response determination in neoadjuvant immunotherapy for patients with NSCLC (19). The mechanisms by which this response to immunotherapy occurs by lymphocytes has not been elucidated either, although some authors hypothesize that peripheral lymphocytes are probably involved in the reinvigoration of the response (19, 20). For these reasons, we propose the study of TCR repertoire and highlight its importance in mediating the response to immunotherapy.

For the first time, we describe longitudinally and spatially the TCR repertoire in patients with NSCLC receiving neoadjuvant chemoimmunotherapy. We also assess its capacity as a possible source for predictive biomarkers of complete pathologic response and its relation with a proimmflamatory state in the tumor microenvironment of CPR patients.

Materials and Methods

Study design and sample collection

All the studies presented here regarding TCR repertoire analysis are exploratory in nature and hypothesis generating and therefore will require validation in larger cohorts. Forty-six patients with resectable stage IIIA from NADIM clinical trial (NCT03081689) were treated with three cycles of nivolumab plus chemotherapy prior to surgery. All patients with enough material were included in the study. Patients were classified in two categories according to their tumor pathologic response: CPR patients (i.e., 0% of viable tumor cells in tumor bed or any lymph node analyzed) and non-CPR patients (i.e., patients with any percentage of viable tumor cells in resection specimens). Informed consent for the collection of research samples and study protocol were approved by the clinical research ethics committee of Hospital Puerta de Hierro in accordance with the International Conference on Harmonization Guidelines on Good Clinical Practice and the Declaration of Helsinki. Written informed consent to participate in the study was obtained from all patients.

Up to 125 samples of peripheral blood ($n = 65$) and tissue ($n = 60$) from these 46 patients were prospectively collected and sequenced to determine their TCR repertoire. TCR sequencing was carried out in peripheral blood mononuclear cell (PBMC) samples collected before ($n = 30$) and after ($n = 35$) neoadjuvant treatment and in tissue samples obtained at diagnosis ($n = 22$) and at surgery ($n = 38$). RNA was used instead of DNA to decrease material input requirements and maximize valid samples for sequencing. Details of all patients, samples, and techniques used are summarized in Supplementary Table S1. In addition, a summary table with the number of paired samples analyzed for each technique and timepoint is shown in Supplementary Table S2. All molecular techniques were carried out in a blind fashion, only the pre- or posttreatment sample origin was known to the researchers conducting the experiments.

RNA extraction

PBMCs were isolated from blood samples by gradient density centrifugation using Lymphoprep (Alere Technologies) and cryopreserved until use. RNA from cryopreserved PBMCs was extracted using Maxwell RSC simply RNA Cells Kit (Promega) as per manufacturer's instructions. RNA from formalin-fixed paraffin-embedded (FFPE) samples of biopsy at diagnosis and surgically resected specimens were extracted with the truXTRAC FFPE DNA Kit (Covaris). RNA quantification was carried out using the Qubit RNA BR Assay Kit (Thermo Fisher Scientific, Catalog No. Q10210) on Qubit apparatus.

TCR library preparation

RNA extracted from PBMCs and FFPE samples was used to prepare the libraries for TCR sequencing. cDNA was obtained from RNA using the SuperScript IV VILO Master Mix (Catalog No. 11756050). RNA input for PBMC-derived libraries was 25 and 100 ng for FFPE-derived libraries. TCR libraries from PBMC samples were done using the Oncomine TCR Beta-LR Assay (Catalog No. A35386). For FFPE-derived RNA samples, TCR libraries were done using the Oncomine TCR Beta-SR Assay (RNA; Catalog No. A39359). For PBMC-derived libraries, equal volumes from 8 samples at 25 pmol/L were pooled for sequencing on an Ion 530 chip. For FFPE-derived libraries, equal volumes from up to 32 samples at 25 pmol/L were combined for sequencing on an Ion 540 chip.

TCR sequencing and data analysis

Once the libraries were templated, they were sequenced in the Ion GeneStudio S5 Series (Thermo Fisher Scientific) and analysis was done via Ion Reporter version 5.12 (Thermo Fisher Scientific). TCR convergence is determined as the aggregate frequency of clones, defined as unique TCRB nucleotide sequences, which shared a variable gene and CDR3 amino acid sequence with at least one other clone. Shannon's diversity was calculated using the formula below, in which p_i is the frequency of clonotype i for the sample with N unique clonotypes (21).

$$\text{Shannon Index } H = -\sum_{i=1}^{N} p_i \log_2(p_i)$$

Evenness describes how evenly distributed is the TCR repertoire, approaching 0 if the repertoire is unbalanced by a reduced number of predominant clones and approaching 1 if the repertoire is balanced, with similar frequencies of all the clones. It is calculated by dividing the Shannon's diversity index by $\log_2(N)$, where N is the total number of detected clones in each sample. Evenness high and low categories were defined using cohort median value (≥0.9077).

Frequency classifications of the clones in the TCR repertoire were done according to their ranked relative abundance in the total T-cell repertoire, named as total clonal space, for each sample. We divided them into top 1%, top 1–2%, top 2–5%, and top >5% (19). In this way, the top 1% clonal space is defined as the aggregate frequencies of the top 1% most frequent clones. Top 1% high and low categories were defined using cohort median value (≥0.166115).

When looking at the dynamics, we refer to contracted or expanded clones as those top 1% clones which their clonal frequency in peripheral blood decreases or increases after treatment.

Jaccard's index was calculated as:

$$Ji = \frac{\text{shared clones } (A+B)}{\text{clones in } A + \text{clones in } B - \text{share clones } (A+B)}$$

Tumor microenvironment lymphocytes and gene expression analysis

Tumor immune cells were identified from FFPE diagnostic biopsies of 11 patients through multiplex immunofluorescence and quantified considering tumor or stroma localization as described previously (1, 22). The immunofluorescence markers used were grouped into two 6-antibody panels and allowed the quantification of: total malignant cells or reactive epithelial cells [CK+ (AE1/AE3+)], malignant cells or reactive epithelial cells PD-L1+ (CK+PD-L1+), total T cells (CD3+), cytotoxic T cells (CD3+CD8+), T cells antigen-experienced (CD3+PD-1+), cytotoxic T cells antigen-experienced (CD3+CD8+PD-1+), T cells PD-L1+ (CD3+PD-L1+), cytotoxic T cells PD-L1+ (CD3+CD8+PD-L1+), T cells antigen-experienced PD-L1+ (CD3+PD-1+PD-L1+), cytotoxic T cells antigen-experienced PD-L1+ (CD3+CD8+PD-1+PD-L1+), total macrophages (CD68+), macrophages PD-L1+ (CD68+PD-L1+), cytotoxic T cells activated (CD3+CD8+Granzyme B+), memory T cells (CD3+CD45RO+), effector/memory cytotoxic T cells (CD3+CD8+CD45RO+), regulatory T cells [(CD3+FoxP3+)-(CD3+CD8+FoxP3+)], and memory/regulatory T cells (CD3+CD45RO+ FoxP3+). Spearman nonparametric test was used for correlations between different cell subpopulations and pretreatment top 1% clonal space.

A single section of FFPE tissue was used to analyze gene expression through the HTG EdgeSeq Precision Immuno-Oncology Panel (HTG

Molecular Diagnostics) following manufacturer's instructions. Ten out of 11 patients sequenced had valid NGS data for further analysis. Using the top 1% clonal space cohort median as threshold (≥0.166115), patients with NGS data were divided in two groups (high and low pretreatment top 1% clonal space).

The Bioconductor DESeq2 packages (version4; ref. 23) was used to perform the differential analysis expression, screening the differential expressed genes (DEGs) between high top 1% and low top 1%. To remove those low expressed genes, we applied an expression filter on row count data, selecting genes with, at least, five counts. A hierarchical clustering heatmap was performed using pheatmap package in R.

A selection of genes with threshold of absolute fold-change ≥ 1 and $P < 0.05$ were recruited to perform the gene ontology (GO) enrichment analysis to identify significant biological processes among those genes. To analyze the processes involved on each group (high top 1% and low top 1%), two groups were established according to their fold-change values: those values ≥1 (upregulated on high top 1% group) and values ≤1 (upregulated on low top 1%). The significant processes were ordered according to their P value, selecting the 25 most significant processes for each group. This analysis was performed with R package bcbioRNASeq (24).

PD-L1 tumor proportion score and TMB assessment

As previously reported, the baseline TMB of FFPE tumor diagnostic samples was assessed using an Ion S5 Sequencer (Thermo Fisher Scientific) with the Oncomine Tumor Mutation Load Assay (Thermo Fisher Scientific) according to the manufacturer's instructions. The commercially available PD-L1 IHC assay PD-L1 IHC 22C3 pharmDx (Dako) was used to assess PD-L1 tumor proportion score (TPS) in FFPE tumor diagnostic samples (1).

Statistical analysis

Graphs were drawn using GraphPad PRISM v.6. and SPSS Statistics v25 was used to analyze the data and determine the statistical significance, considered by an overall P value <0.05. Statistical significance was adjusted for multiple testing by Bonferroni correction when appropriate and was indicated in figure caption. Two-tailed, nonparametric Mann–Whitney U test was performed to compare CPR versus non-CPR groups. Wilcoxon matched-pairs signed rank test was adopted to make comparisons between pre- and post-neoadjuvant treatment in paired samples. Spearman rank nonparametric test was used for variable correlations. High and low pretreatment top 1% clonal space patient groups were defined using the pretreatment TCR cohort median ($n = 22$). Contingency table analysis when comparing top 1% high and low patients with clinicopathologic features was done using Fisher exact test or Chi-square test. The ROC curve analysis was done to determine the association of the variables studied with therapy pathologic response. Regarding gene expression analysis, a multiple testing correction was performed to reduce the number of false positives, using Benjamini–Hochberg procedure and an adjusted $P < 0.05$ was considered statistically significant.

Availability of data

The datasets supporting this study are available from the corresponding authors upon request. Raw sequencing data are not freely available due to lack of specific authorization, regarding potential relevant germline information release, present in the original consent form signed by the patients during trial enrollment. However, raw data are available upon request and complete TCR clone lists identified in pretreatment or posttreatment samples can be found in Supplementary Files S1 and S2, respectively.

Results

Pretreatment tissue TCR evenness is associated with pathologic response to neoadjuvant chemoimmunotherapy

Forty-six patients with resectable stage IIIA were treated with three cycles of nivolumab plus chemotherapy prior to surgery; 41 of them underwent surgical resection. The clinicopathologic characteristics of the patients analyzed are shown in **Table 1**. PBMC samples collected before (pre-) and after (post-) neoadjuvant treatment and tumor samples obtained at diagnosis (pre-) and at surgery (post-) were subjected to TCR sequencing (Supplementary Table S1). From 77 tissue samples collected, we obtained valid TCR data for 60 (78%); three samples did not have sufficient tissue for RNA extraction and 14 did not yield enough RNA quantity for further analysis, however, all samples with enough RNA quantity generated valid NGS data. On the contrary, from 65 blood samples collected, we were able to obtain valid TCR data in all cases (100%).

As a first approach, TCR repertoire-derived metrics were analyzed. Regarding blood, there were no differences between CPR and non-CPR patients in both pre- or posttreatment PBMC samples in terms of clones sequenced, convergence, evenness, and diversity (**Fig. 1A**). Also, there were no differences between pre- and posttreatment PBMC samples in all patients nor stratifying by pathological response for these parameters (**Fig. 1A**).

However, when comparing tissue samples at diagnosis, we found that CPR patients had significantly lower TCR evenness in the TCR repertoire than non-CPR patients ($P = 0.010$), reflecting a skewed repertoire in complete pathologic responders (**Fig. 1B**). No differences were found in the other TCR metrics. In contrast, there were no differences in evenness in surgery samples. Focusing on the effect of neoadjuvant treatment, an increase in evenness ($P = 0.028$), and a decrease in number of clones ($P = 0.037$), between pre- and post-treatment samples seems to be observed in patients who had CPR, that were not considered statistically significant after Bonferroni's correction (**Fig. 1B**).

Extensive analysis to define which ranges of clones were responsible for CPR and non-CPR TCR evenness differences was done. The top 1% most common clones occupied higher clonal space, with respect to the total repertoire, in CPR patients than in non-CPR patients ($P = 0.00015$; **Fig. 1C**). Opposite results were found for clones below the top 5% most common clones ($P = 0.001$; **Fig. 1C**). However, these differences were lost in surgery samples, presenting CPR and non-CPR patients similar clonal space values for all clonal ranges. Evaluating treatment effect, although a decrease in the clonal space occupied by the top 1% seems to occur in posttreatment compared with pretreatment samples, this was not statistically significant ($P = 0.043$; **Fig. 1C**).

Pretreatment tissue TCR evenness and top 1% outperform TMB and PD-L1 identifiying patients who achieve CPR

The ability of these two potential tissue biomarkers to potentially predict the pathologic response of these patients was analyzed. The AUC ROC for TCR evenness to distinguish between CPR and non-CPR was 0.844 [95% confidence interval (CI), 0.667–1.000; $P = 0.011$]. An evenness value lower than 0.863 showed 50% sensitivity and 100% specificity identifying patients that will achieve CPR, and therefore, will be potentially free of disease at the time of surgery (**Fig. 2A**). Determination of top 1% clonal space categorizes CPR and non-CPR patients with more accuracy than evenness, showing an AUC of 0.967 (95% CI, 0.897–1.000; $P = 0.001$; **Fig. 2A**). Top 1% clonal space higher

Table 1. Clinicopathologic characteristics of patients and their association with pretreatment tissue top 1% clonal space.

Clinicopathologic characteristics	Complete molecular cohort ($n = 44$)	Pretreatment TCR analysis cohort ($n = 22$)	Top 1% clonal space high ($n = 11$)	Top 1% clonal space low ($n = 11$)	P value (top 1% clonal space high vs. low)
Age (years)					0.428[a]
Median (IQR)	62 (58.5–70)	65 (59–71)	68 (59–71)	64 (56–71)	
Sex					0.586[b]
Male	32 (72.73)	18 (81.81)	8 (72.73)	10 (90.91)	
Female	12 (27.27)	4 (18.18)	3 (27.27)	1 (9.09)	
Smoking status					1.000[b]
Former	23 (52.27)	10 (45.45)	5 (45.45)	5 (45.45)	
Smoker	21 (47.73)	12 (54.55)	6 (54.55)	6 (54.55)	
Histology					0.475[c]
Squamous	15 (34.09)	10 (45.45)	4 (36.36)	6 (54.55)	
Adenocarcinoma	25 (56.82)	11 (50.00)	6 (54.55)	5 (45.45)	
NOS	4 (9.09)	1 (4.55)	1 (9.09)	0 (0)	
Nodal stage					0.338[b]
N0	9 (20.45)	6 (27.27)	4 (36.36))	2 (18.18)	
N1	3 (6.82)	0 (0)	0 (0)	0 (0)	
N2	32 (72.73)	16 (72.73)	7 (63.64)	9 (81.82)	
Path response					0.006[c]
CPR	25 (56.82)	10 (45.45)	9 (81.82)	1 (9.09)	
MPR	8 (18.18)	3 (13.64)	0 (0)	3 (27.27)	
IPR	7 (15.91)	6 (27.27)	1 (9.09)	5 (45.45)	
Non-resected	4 (9.09)	3 (13.64)	1 (9.09)	2 (18.18)	

Note: The data shown correspond to number and (%) or median and (IQR). Complete molecular cohort consisted in all patients from who at least one molecular analysis was done (TMB, PD-L1, TILs, HTG, or TCR determination). Pretreatment TCR cohort was composed of all patients from whom TCR metrics were determined in pretreatment tissue sample. Patients with TCR determination in pretreatment tissue were classified as top 1% high or low according to cohort median (0.166115). Abbreviations: IPR, minor pathologic response; IQR, interquartile range; MPR, major pathologic response; NOS, not otherwise specified.
[a]P value was calculated using the Mann–Whitney U test.
[b]P value was calculated using Fisher exact test.
[c]P value was calculated using Chi-square test.
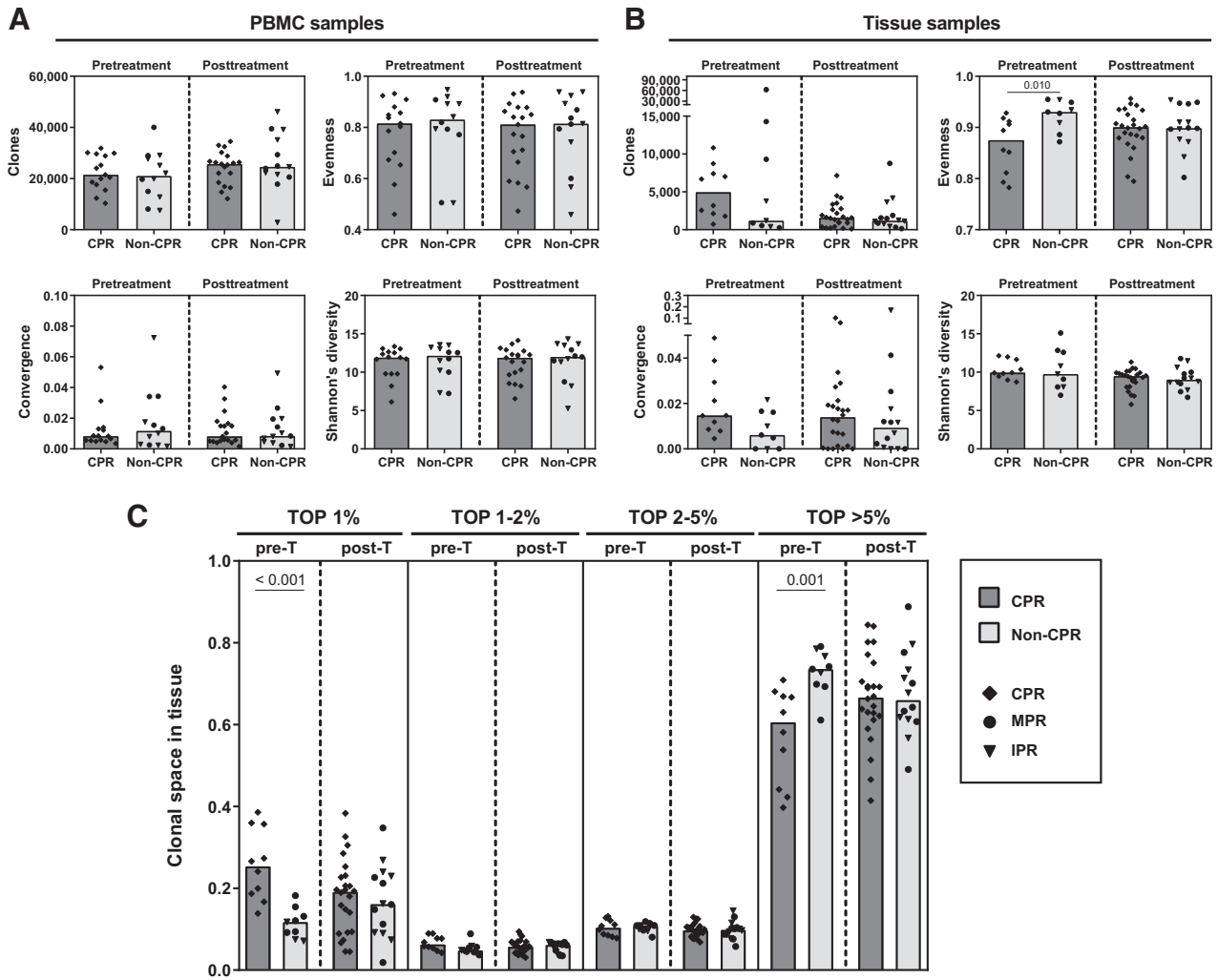
Figure 1.
Pretreatment tissue TCR evenness is associated with pathologic response to neoadjuvant chemoimmunotherapy. **A,** Differences in metrics derived from TCR repertoire analysis (such as number of clones, evenness, convergence, and Shannon's diversity index) in peripheral blood samples between CPR and non-CPR patients at pre- and post-neoadjuvant treatment. Pretreatment (pre-T) CPR patients, $n = 15$; pre-T non-CPR patients, $n = 12$; posttreatment (post-T) CPR patients, $n = 19$; post-T non-CPR patients, $n = 13$. **B,** Differences in metrics in tissue samples between CPR and non-CPR patients. Pre-T CPR patients, $n = 10$; pre-T non-CPR patients, $n = 9$; post-T CPR patients, $n = 24$; post-T non-CPR patients, $n = 14$. Comparisons were done between CPR and non-CPR patients and between pre- and posttreatment timepoints. **C,** Clonal space occupied by each of the percentage rank (top 1%, top 1–2%, top 2–5%, and top > 5%) of the total repertoire in tissue samples. Comparisons between CPR and non-CPR patients are shown for each rank. Pre-T CPR patients, $n = 10$; pre-T non-CPR patients, $n = 9$; post-T CPR patients, $n = 24$; post-T non-CPR patients, $n = 14$. Each patient is represented by a black symbol. $P < 0.0125$ was considered statistically significant after Bonferroni's correction for multiple tests. Only significant differences after Bonferroni's correction are shown.

than 0.1842 showed 80% sensitivity and 100% specificity identifying patients that will achieve CPR after chemoimmunotherapy. Out of the 19 total patients from our cohort with valid data, we were able to classify correctly 8/10 of those with CPR using this cut-off. No association between pretreatment tissue top 1% clonal space using the cohort median as threshold with age, sex, smoking status, histology, or nodal stage at diagnosis was found (**Table 1**).

We next compared the ability of TCR evenness and top 1% clones with PD-L1 TPS and TMB to potentially predict CPR patients. The AUC ROCs for PD-L1 TPS and TMB to distinguish CPR and non-CPR patients were 0.767 (95% CI, 0.578–0.955; $P = 0.026$) and 0.550 (95% CI, 0.308–0.792; $P = 0.687$), respectively (**Fig. 2A**). These results indicate that both evenness and top 1% showed better sensitivity and

specificity to classify patients achieving CPR after neoadjuvant chemoimmunotherapy than the commonly used PD-L1 and TMB.

Regarding survival, although the number of patients is limited and due to the efficacy of the therapy the number of events is small, patients with high pretreatment tissue top 1% clonal space seem to show a better prognosis both in their PFS ($P = 0.053$) and OS ($P = 0.059$; **Fig. 2B**). Thus, in the low top 1% group 5 patients have progressed and 3 of them have died, whereas in the high top 1% group only 1 patient has progressed without any death. These patterns are not observed for evenness, PD-L1, or TMB using median values as thresholds (Supplementary Fig. S1A).

We also assessed the relationships between TCR evenness, top 1%, PD-L1 TPS, and TMB analyzing the correlations between them.
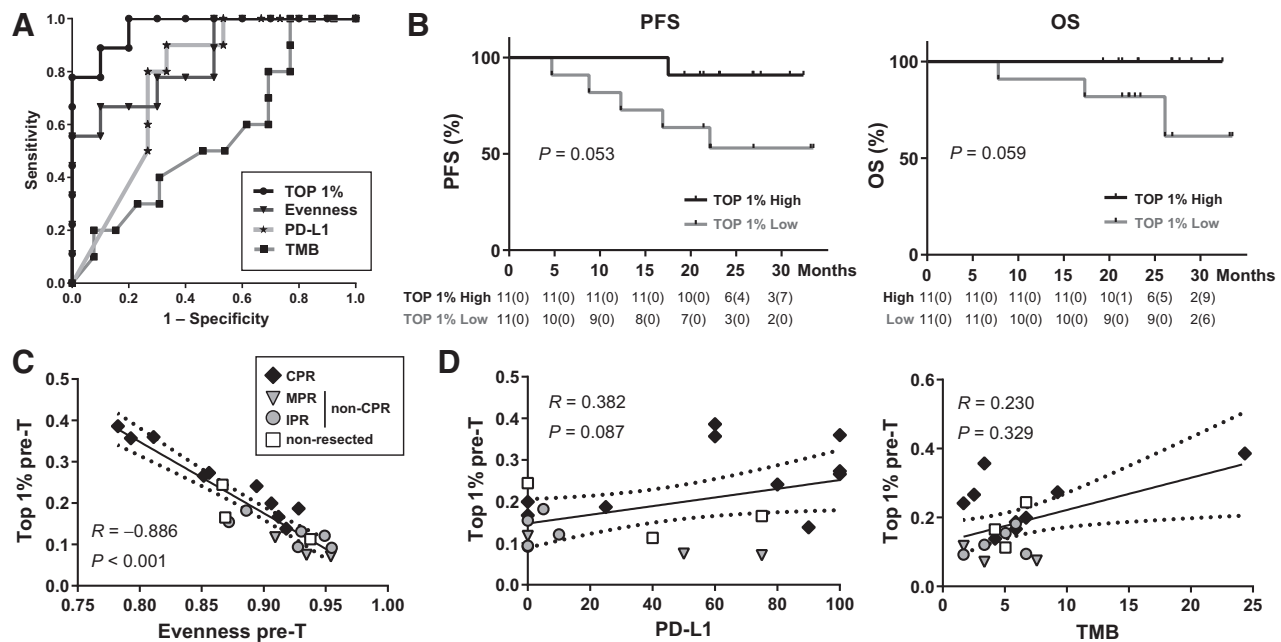
Figure 2.

Pretreatment tissue TCR evenness and top 1% could be better predictors of pathologic response than TMB and PD-L1. **A,** ROC curve analysis for TMB (square, $n = 23$), PD-L1 (asterisk, $n = 25$), evenness (triangle, $n = 19$), and top 1% (dot, $n = 19$) determined in pretreatment tissue samples. **B,** PFS and OS percent survival stratified by pretreatment top 1% clonal space high and low patients ($n = 22$). **C,** Correlation between clonal space occupied by top 1% clones and evenness in pretreatment tumor samples ($n = 22$; CPR, $n = 10$; non-CPR, $n = 9$; nonresected, $n = 3$). **D,** Correlation between clonal space occupied by the top 1% clones and PD-L1 in pre-T tissue samples ($n = 21$; CPR, $n = 10$; non-CPR, $n = 8$; nonresected, $n = 3$) and correlation between frequency of the top 1% clones and TMB in pretreatment tissue samples ($n = 20$; CPR, $n = 9$; non-CPR, $n = 8$; nonresected, $n = 3$). Each patient is represented by a dark gray (CPR), light gray (non-CPR), or white (nonresected) symbol. The black line indicates the linear regression line, and the dotted lines indicate the upper and lower boundaries of the 95% CI.

Evenness and top 1% clonal space were strongly negatively correlated ($R = -0.886$; $P < 0.001$; **Fig. 2C**). However, there was no correlation between top 1% clonal space and PD-L1 or TMB ($R = 0.382$, $P = 0.087$; $R = 0.230$, $P = 0.329$; **Fig. 2D**) nor between evenness and PD-L1 or TMB ($R = -0.359$, $P = 0.109$; $R = -0.241$, $P = 0.306$; Supplementary Fig. S1B), strengthening the independent value of these biomarkers.

The presence of any mutations of potential clinical relevance, specifically *KEAP1* ($n = 3$), *EGFR* ($n = 1$), *TP53* ($n = 9$), *KRAS* ($n = 3$), and *HNF1A* ($n = 4$) in this cohort, was not associated with changes in tumor top 1% clonal space levels (Supplementary Fig. S1C; Supplementary Tables S1 and S3).

Tissue TCR evenness and top 1% clonal space are independent of main technical parameters

To assess the robustness of tissue TCR repertoire evenness and top 1% clonal space parameters, we tested whether different common technical factors (i.e read depth, identified clones, tissue origin, and library preparation) could influence these putative biomarkers.

No correlation between reported read count and evenness ($R = -0.079$; $P = 0.748$) or tissue top 1% clonal space ($R = 0.384$; $P = 0.104$) was observed (Supplementary Fig. S2A). In addition, there were no differences in read counts between samples of CPR and non-CPR patients at diagnosis ($P = 0.182$) or surgery ($P = 0.777$; Supplementary Fig. S2B). Also, no correlation was found between the number of clones detected and evenness ($R = 0.149$; $P = 0.542$) or top 1% clonal space ($R = 0.193$; $P = 0.429$; Supplementary Fig. S2C).

Furthermore, these biomarkers were not strongly influenced by biopsy's origin. No differences were found between tumor or lymph node biopsies, for both evenness or top 1% clonal space (Supplementary Fig. S2D). Also, the differences seen in the frequency of the top 1% were maintained regardless of the origin of the sample. Patients with CPR have a higher frequency of the top 1% than non-CPR patients in both tumor tissue samples ($P = 0.030$) and in lymph node samples ($P = 0.029$; data not shown). Finally, we also checked that these metrics and the clonal reproducibility did not significantly vary between different libraries made from the same sample or within technical sequencing replicates from the same library. TCR evenness and top 1% were stable across technical replicates (Supplementary Fig. S3A). Clonal reproducibility was almost perfect between sequencing replicates, reaching a Jaccard's index near 1 for all clonal ranges. However, the clonal reproducibility between libraries was only maintained for top 1% and top 1% to 2%, decreasing for top 2% to 5% and being almost gone for clones below the 5% most common clones (Supplementary Fig. S3B).

CPR patients showed a selective expansion of pretreatment tissue top 1% clones in peripheral blood

In view of the importance of the top 1% frequency-ranked clones present in pretreatment tissue samples, we studied the relevance of this top 1% in the different compartments, deepening in the study of their individual dynamics in peripheral blood and tissue considering whether they were expanded or contracted during neoadjuvant treatment.

As a first approach in blood, we found no statistically significant differences between CPR and non-CPR patients in the clonal space occupied by the top 1% clones of diagnostic tissue in pre- or posttreatment PBMC samples (pretreatment, $P = 0.234$; posttreatment,
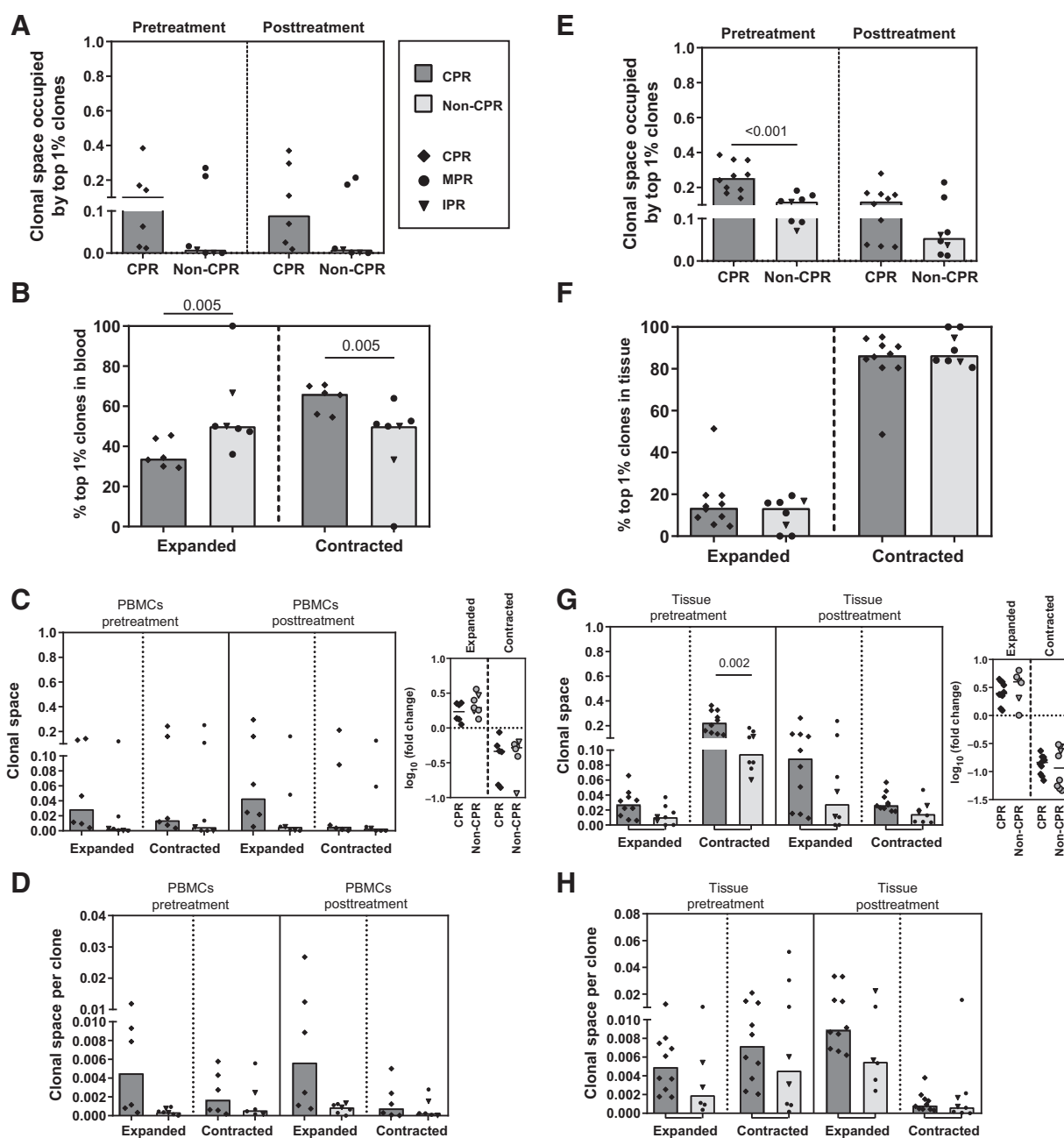
Figure 3.
CPR patients showed a selective expansion of tissue top 1% clones in peripheral blood. **A,** Clonal space occupied by the top 1% tissue pre-T clones in pre- and posttreatment PBMC samples. Comparisons between CPR and non-CPR patients in pre- and posttreatment timepoints are shown ($n = 13$; CPR, $n = 6$; non-CPR, $n = 7$). **B,** Percentage of top 1% tissue pre-T clones that were peripherally expanded or contracted (known as dynamic clones). Comparisons between CPR and non-CPR patients are shown ($n = 13$; CPR, $n = 6$; non-CPR, $n = 7$). **C,** Clonal space occupied by dynamic clones in peripheral repertoire: PBMCs pre-T and PBMCs post-T. Expressed as frequency of clonal space occupied by the top 1% tissue pre-T clones and fold change between pre- and posttreatment timepoints. Comparisons between CPR and non-CPR patients are shown ($n = 13$; CPR, $n = 6$; non-CPR, $n = 7$). **D,** Median contribution of peripherally expanded ($n = 13$; CPR, $n = 6$; non-CPR, $n = 7$) or contracted clones ($n = 12$; CPR, $n = 6$; non-CPR, $n = 6$) in pre- and posttreatment peripheral blood. Comparisons between CPR and non-CPR patients are shown. **E,** Clonal space occupied by the top 1% tissue pre-T in pre- and posttreatment tissue samples. Comparisons between CPR and non-CPR patients in pre- and posttreatment timepoints are shown ($n = 18$; CPR, $n = 10$; non-CPR, $n = 8$). **F,** Percentage of top 1% tissue pre-T clones that were intratumorally expanded or contracted. Comparisons between CPR and non-CPR patients are shown ($n = 18$; CPR, $n = 10$; non-CPR, $n = 8$). **G,** Clonal space occupied by top 1% dynamic clones in tissue: tissue pre-T and tissue post-T. Expressed as frequency of clonal space occupied and fold change between pre- and post-timepoints. Comparisons between CPR and non-CPR patients are shown ($n = 18$; CPR, $n = 10$; non-CPR, $n = 8$). **H,** Median contribution of intratumorally expanded ($n = 16$; CPR, $n = 10$; non-CPR, $n = 6$) or contracted clones ($n = 18$; CPR, $n = 10$; non-CPR, $n = 8$) in pre- and posttreatment peripheral blood. Comparisons between CPR and non-CPR patients are shown. Each patient is represented by a symbol. $P < 0.0125$ was considered statistically significant after Bonferroni's correction for multiple tests. Only significant differences after Bonferroni's correction are shown.

$P = 0.059$). Similarly, there was also no significant changes after treatment in the clonal space of this pretreatment tissue top 1% clones in blood for both CPR and non-CPR patients (**Fig. 3A**).

We also evaluated the percentage of peripherally expanded or contracted pretreatment tissue top 1% clones. Patients achieving CPR showed statistically significant lower percentage of expanded clones and consequently, higher percentage of contracted clones compared with non-CPR patients ($P = 0.005$; **Fig. 3B**). However, there were no differences in the clonal space occupied by expanded or contracted pretreatment tissue top 1% clones between pathologic response groups in pre- or posttreatment PBMC samples nor in their fold changes associated (**Fig. 3C**).

Because the percentage of expanded clones in CPR patients was lower than in non-CPR, but the clonal space remained similar, we decided to evaluate the individual contribution of those clones to the clonal space. To do this, we normalized the clonal space by the number of clones that were expanded or contracted, thus comparing the average clonal space per clone between CPR and non-CPR patients. The tissue top 1% clones that were expanded in the blood of CPR patients seems to have larger average size per clone than their non-CPR counterparts; both in the pre- ($P = 0.022$) or post- ($P = 0.051$) PBMCs' clonal space (**Fig. 3D**).

Concerning their implication in tissue, the clonal space occupied by the pretreatment top 1% clones in tissue samples was significantly reduced after treatment for all patients ($P = 0.005$). However, stratifying by pathological response, only CPR patients showed a decrease (CPR patients, $P = 0.013$; non-CPR patients, $P = 0.208$; **Fig. 3E**). In addition, the space occupied by the pretreatment top 1% tissue clones seems to be higher in CPR patients compared with non-CPR patients after treatment, although no statistically significant differences were seen ($P = 0.237$).

When looking at their intratumoral dynamics, we observed that more than 80% of them were contracted in post-neoadjuvant treatment tissue. Unlike blood, no differences were observed in tissue top 1% dynamics between CPR and non-CPR patients (**Fig. 3F**). Same as previously shown with PBMC samples, the clonal space occupied by expanded clones nor the fold change between pre- and posttreatment tissue, showed differences between CPR and non-CPR patients (**Fig. 3G**). In addition, there was a higher clonal space occupied by contracted clones in tissue pretreatment in CPR patients compared with non-CPR ($P = 0.002$; **Fig. 3G**). However, no differences were seen in the average clonal space occupied by each clone in pre- and posttreatment tissue, in CPR or non-CPR patients (**Fig. 3H**).

Tumors with high pretreatment top 1% clonal space showed an immune reactive gene expression profile

To understand what characterizes the tumors with high or low top 1% clonal space, we analyzed the relationship of this biomarker with the pretreatment tumor immune infiltrate and the gene expression profile.

In terms of immune cell content, no association was found between top 1% clonal space and tumor, stroma, or total levels of any immune cell subpopulations analyzed (data not shown). Only a weak correlation was found between T lymphocytes infiltrating the tumor (CD3+ cells) and the clonal space of the top 1% ($R = 0.609$, $P = 0.047$) that was not considered statistically significant after multiple comparisons correction (**Fig. 4A**). However, stratifying between high and low top 1% clonal space tumors, using cohort median as cutoff, no differences were found in CD3+ levels (**Fig. 4A**).

Despite the low number of cases analyzed, the RNA sequencing (RNA-seq) results showed a differential gene expression profile for tumors with high or low top 1% clonal space, as shown in the hierarchical heatmap (**Fig. 4B**). Nearly 200 genes were differentially expressed in high compared with low top 1% tumors (**Fig. 4C**). Specifically, 139 genes were upregulated, including *IFNg* (Log2FC 1.14, adjusted P value $= 0.022$), *IL2* (Log2FC 1.78, adjusted P value < 0.001), and *IL13* (Log2FC 2.16, adjusted P value < 0.001). Conversely, 53 genes were downregulated, including *VEGFC* (Log2FC -1.39, adjusted P value $= 0.008$), *MAPK1* (Log2FC -1.30, adjusted P value $= 0.008$), or *IGF1R* (Log2FC -1.31, adjusted P value < 0.001). A complete list of differentially expressed genes can be found at Supplementary Table S4.

Finally, to identify the main biological processes of differentially expressed genes in tumors with high pretreatment top 1% clonal space, GO enrichment analysis was carried out (Supplementary Table S5). Top 25 terms for upregulated genes include processes such as: positive regulation of immune effector process (GO:0002699), positive regulation of cell killing (GO:0031343), or regulation of receptor signaling pathway via JAK-STAT (GO:0046425). On the other hand, top 25 terms for downregulated genes include processes such as: epithelial cell proliferation (GO:0050673), cell-cycle arrest (GO:0007050), positive regulation of angiogenesis (GO:0045766), negative regulation of extrinsic apoptotic signaling pathway (GO:2001237), or positive regulation of protein serine/threonine kinase activity (GO:0071902; **Fig. 4D**).

Shared and newly emergent posttreatment top 1% clones are not informative of patient response

To reveal possible response mechanisms, we decided to analyze also the role of the clones belonging to the top 1% posttreatment tissue according to whether they belong to the pretreatment top 1%, pretreatment non–top 1%, or were newly emerging clones (NEC; i.e., not detected in pretreatment tissue).
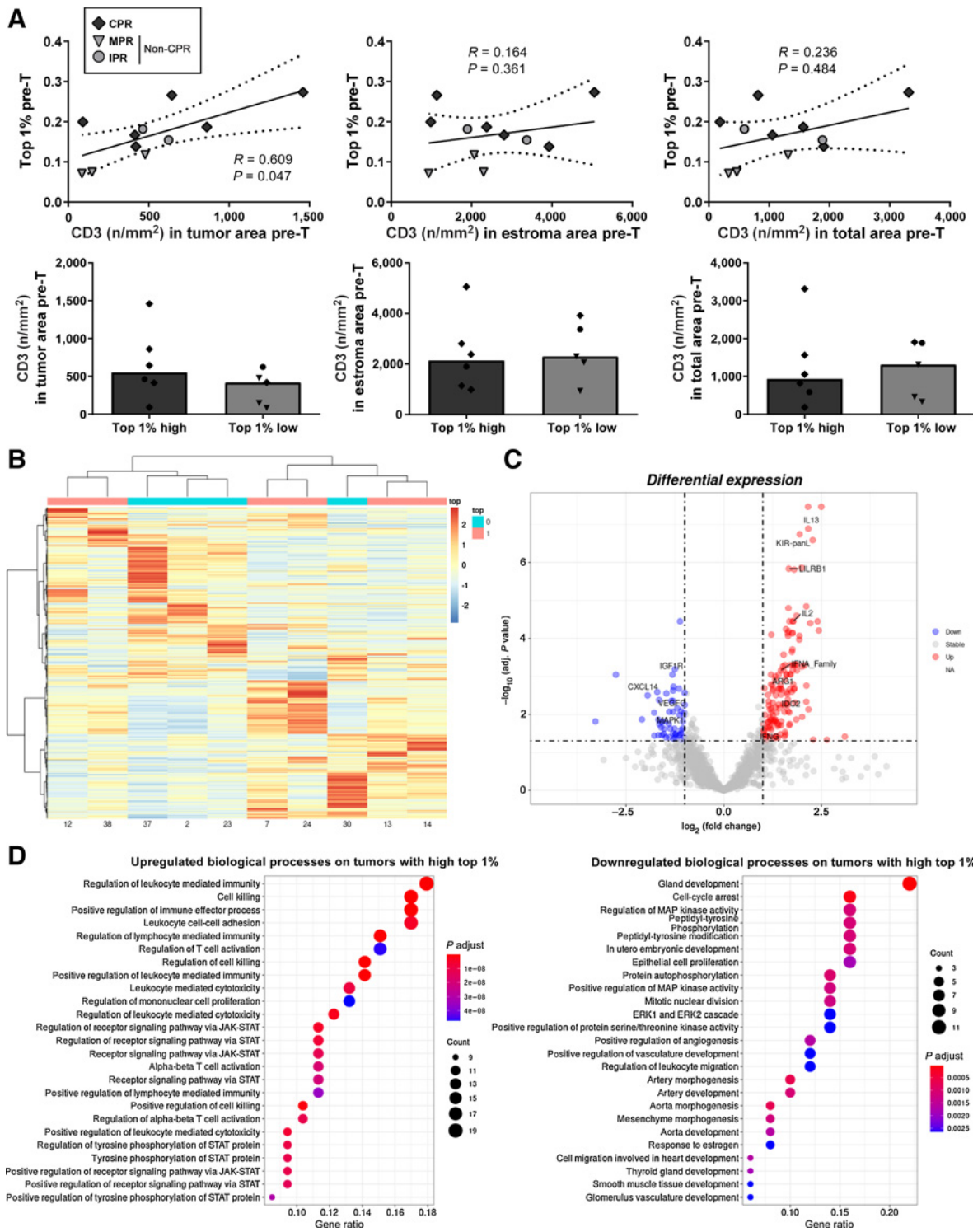
Posttreatment tissue top 1% clonal space analysis showed no statistically significant differences between these categories ($P = 0.073$), however the median clonal space of non–top 1% pretreatment clones doubles the clonal space of NEC in posttreatment tissue ($P = 0.09$; **Fig. 5A**). Anyhow, no differences between CPR and non-CPR were observed in the relative space of these clone subgroups (**Fig. 5B**).

To determine the specific relevance of the pretreatment top 1% clones, their clonal space was compared with the rest of the clones (i.e., the sum of the non–top 1% and NEC clones), showing the latter category larger values, occupying near 70% of the posttreatment top 1% clonal space ($P = 0.010$; **Fig. 5C**).

Regarding NEC, their clonal space was compared with that occupied by pretreatment shared clones. The clonal space of shared clones was higher than that of NEC, occupying near 80% of the posttreatment top 1% clonal space ($P = 0.020$; **Fig. 5D**).

To analyze in blood the dynamics of the top 1% clones of posttreatment samples, we selected those patients from whom we had paired samples of the four compartments (tissue and blood at the pre- and posttreatment timepoints, $n = 12$). Clonal space of tissue shared clones were not altered in blood after treatment (Supplementary Fig. S4A), being this behavior similar between CPR and non-CPR patients (Supplementary Fig. S4B). Concerning NEC, an increase in their clonal space in blood after treatment was observed ($P = 0.018$; Supplementary Fig. S4C). Analyzing it by response, it seems that this increase is mostly produced in non-CPR patients, showing a trend for higher NEC clonal space in posttreatment blood compared with CPR patients ($P = 0.020$; Supplementary Fig. S4D).

Figure 4.
Immune cells and gene expression analysis of tumors with high or low top 1% clonal space. **A,** Correlation between CD3+ tumor-infiltrating lymphocytes (cells per mm^2) and top 1% clonal space in pretreatment tissue. Comparisons between high top 1% and low top 1% patients are shown. $P < 0.001$ was considered statistically significant after Bonferroni's correction for multiple tests. **B,** Hierarchical clustered heatmap showing the expression patterns of all genes analyzed across tumors with high (pink) and low (cyan) top 1% clonal space. The red boxes indicate the upregulated genes, and the blue boxes indicate downregulated genes. **C,** Volcano plot showing the log$_{10}$ of adjusted P value and log$_2$ fold change of all genes studied. Red (upregulated) and blue (downregulated) dots represent genes with log$_2$ fold change >|1| and statistically significant (adjusted P value <0.05). **D,** Dot plots of top 25 enriched GO pathways for downregulated and upregulated genes in tumor with high top 1% clonal space versus tumors with low top 1% clonal space.
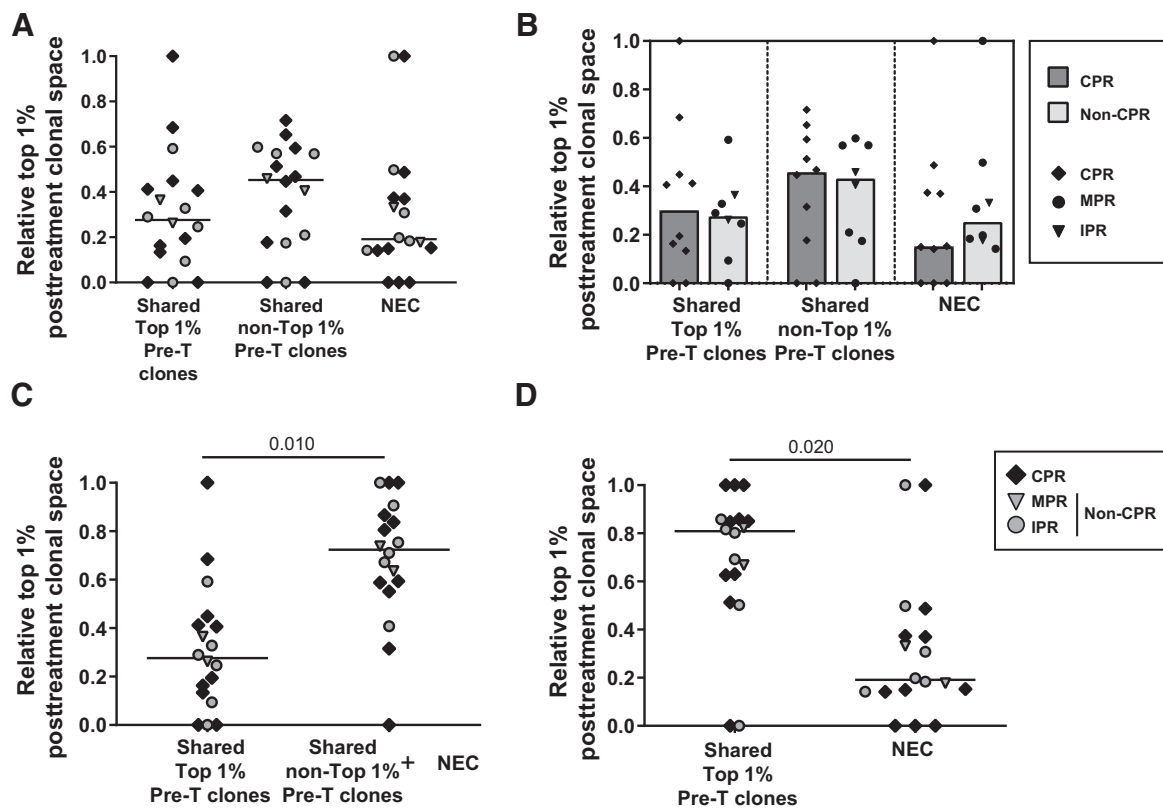
Figure 5.
Composition of top 1% clones of surgical specimens. **A,** Relative top 1% posttreatment clonal space occupied by clones shared between pre- and posttreatment, belonging to the top 1% pre-T tissue or non–top 1%, and by NEC ($n = 18$; CPR, $n = 10$; non-CPR, $n = 8$). Comparisons between shared top 1% pre-T clones, shared non–top 1% pre-T clones, and NEC were done. **B,** Relative top 1% posttreatment clonal space occupied by clones shared between pre- and posttreatment, belonging to the top 1% pre-T tissue or non–top 1%, and by NEC stratified by response ($n = 18$; CPR, $n = 10$; non-CPR, $n = 8$). Comparisons between CPR and non-CPR patients were done. **C,** Comparison of the relative top 1% posttreatment clonal space occupied between shared top 1% clones and non–top 1% plus NEC ($n = 18$). **D,** Comparison of the relative top 1% posttreatment clonal space occupied between total shared clones and NEC ($n = 18$). Each patient is represented by a symbol. $P < 0.05$ was considered statistically significant. Only significant differences are shown.

Discussion

There is a need for predictive biomarkers since neither PD-L1 nor TMB are capable of accurately predicting the response to chemoimmunotherapy in patients with advanced NSCLC (5–7), or neoadjuvant chemoimmunotherapy in locally advanced patients (1, 2). In this study, we performed TCR sequencing in peripheral blood and tissue samples from patients enrolled in NADIM trial (NCT03081689), at both pre- and post-neoadjuvant treatment timepoints. With this approach, we have shown for the first time a relationship between an uneven TCR repertoire in tissue samples at diagnosis and the complete pathologic response in NSCLC patients treated with chemoimmunotherapy.

We hypothesized that this uneven repertoire in CPR patients could be caused by a small number of dominating clones in the total repertoire. When looking to the most frequently ranked clones, we saw that the top 1% clones occupied higher clonal space in complete responder patients than in non–complete responders. Altogether, we have demonstrated that these two novel biomarkers derived from the TCR repertoire analysis could predict, with higher accuracy than PD-L1 and TMB, patients that will be free of disease at time of surgery due to their association with CPR after neoadjuvant chemoimmunotherapy.

In this way, the study of the pretreatment tissue top 1% clonal space as potential biomarker is encouraging; it reflects tumor immunogenicity and is strongly associated with tumor response being technically robust (21) and affordable considering turn-around times and costs. Thus, if its value is confirmed in larger cohorts with longer follow-ups for survival analysis, we believe that the analysis of the top 1% clonal space could be implemented in the clinic. This could allow the personalization of the follow-up and treatment of patients with low top 1% clonal space, who would presumably not achieve CPR, as well as would enable studies to determine the value of surgery in patients that will achieve CPR, that likely would present high top 1% clonal space at diagnosis. However, limitations similar to those of TMB, such as standardization between platforms and laboratories, as well as democratization of NGS access, would have to be solved for an effective application in clinical practice. The role of the most frequent clones as biomarkers was also assessed in other studies, in which a higher frequency of these top-ranked clones in peripheral blood was associated with higher PFS rates at 9 months in patients treated with immunotherapy (12) and that a higher frequency of the top 1% clones present at resection was associated with MPR (19). However, this is the first time that baseline TCR parameters showed an association with CPR after chemoimmunotherapy.

We have shown that tumors with higher top 1% clonal space presented—despite having similar levels of PD-L1, TMB, or TIL populations—a higher pro-inflammatory profile reflected by upregulation of biological processes such as leukocyte-mediated immunity, cell killing, and T-cell activation among others. This stronger immunogenic profile could explain the repertoire imbalance and greater pathologic responses, since in such a permissive microenvironment the specific activation and clonal expansion after antigen recognition of some antitumoral T-cell clones would be more easily allowed (25, 26). In turn, it seems that this repertoire imbalance does not depend exclusively on the TMB of these tumors, but existing modifying elements between the mutations and their ability to elicit an immune response [i.e., neoantigen presentation (27, 28), or immunosuppressive microenvironment factors (29)], that the study of TCR repertoire would consider, but TMB alone would not.

Concerning the mechanism and involvement of pretreatment tissue top 1% clones in the response, there are different options that are compatible with each other.

On the one hand, it is possible that these clones were not involved in the response. Thus, new clones or clones belonging to the non–top 1% category would participate in the response, as would support: the increase of tissue NEC in blood posttreatment, the loss of clonal space of top 1% pretreatment clones in posttreatment tissue, and the rise of clonal space of pretreatment non–top 1% clones and NEC in top 1% clonal space of posttreatment tissue (which combined account for more clonal space than that of the pretreatment top 1% clones). However, NEC in the top 1% posttreatment tissue seem to occupy half of the space that pretreatment non–top 1% clones do, indicating a greater importance of reinvigoration of preexisting tumor clones below the top 1% than of the emergence of new clones. In any case, the fact that no differential behavior is observed between responses, reinforces that the NEC and non–top 1% clones do not seem to have a specific role to achieve CPR, however it does not rule out their possible participation in responses.

On the other hand, we have shown how this top 1% remained in tissue posttreatment and was also present in the blood. Thus, the possible role of these clones in the response may be exerted through tissue or peripheral mechanisms. In terms of tissue mechanisms, despite this drop of pretreatment tissue top 1% clones, they still account for 10% to 20% of the total posttreatment clonal space (showing a tendency to be more relevant in CPR patients) and occupy near 30% of the posttreatment top 1% clonal space. Furthermore, this role may have been underestimated given that, at the time of surgery, there was a reduction of T cells probably related to tumor clearance (1). Thus, we cannot rule out the importance of reinvigoration of top 1% in tumor elimination (30). Regarding the role of pretreatment tissue top 1% clones in the peripheral response, we have seen that in our patients the clones identified in tissue are found in blood and are maintained after treatment. Furthermore, CPR patients showed a selective expansion of pretreatment tissue top 1% clones in peripheral blood compared with non-CPR patients. This could indicate peripheral immunosurveillance, responsible for eliminating possible relapses at systemic level, which could explain the high survival rate of patients with CPR (1) and the absence of deaths in the high top 1% group. In this regard, other authors have previously described the clonal changes in the peripheral TCR repertoire after immunotherapy, and identified clones that expanded or contracted peripherally after treatment (12, 15, 19, 20).

Finally, further studies are needed to overcome the limitations of our study, including but not limited to: the number of patients, the lack of in-between samples (19), the lack of a control group and a validation cohort, and the phenotype and antigen specificity of the sequenced T cells (31).

Conclusions

In conclusion, baseline tissue TCR evenness and top 1% clonal space are associated with complete pathologic response to neoadjuvant chemoimmunotherapy. In addition, although we cannot rule out the role of new clones and the tissue reinvigoration of pretreatment clones, we describe the relevance of the peripheral selective expansion of tissue top 1% clones to achieve complete pathological response. Future studies are warranted in larger cohorts overcoming our limitations to validate the relevance of the TCR repertoire analysis.

Authors' Disclosures

A. Cruz-Bermúdez reports non-financial support from Thermo Fisher Scientific during the conduct of the study. E. Nadal reports grants, personal fees, and non-financial support from Bristol-Myers Squibb, Roche, and Pfizer; personal fees and non-financial support from Merck Sharp & Dohme, Takeda, AstraZeneca, Lilly, and Boehringer Ingelheim; grants and personal fees from Merck Serono; and personal fees from Amgen and Bayer outside the submitted work. A. Insa reports personal fees from Bristol, Boehringer Ingelheim, Roche, MSD-Merck, Amgen, and Takeda outside the submitted work. M.R. García Campelo reports personal fees from BMS during the conduct of the study, as well as personal fees from MSD, Roche, AstraZeneca, Takeda, Pfizer, Janssen, Novartis, and Lilly outside the submitted work. M. Lázaro reports personal fees from BMS, Roche, and MSD outside the submitted work. M. Dómine reports personal fees from AstraZeneca, BMS, Boehringer Ingelheim, MSD, Pfizer, Roche, and Takeda outside the submitted work. M. Majem reports personal fees from BMS, MSD, Roche, Sanofi, AstraZeneca, and Boehringer Ingelheim outside the submitted work. D. Rodríguez-Abreu reports personal fees from Bristol Myers Squibb, Novartis, MSD, Eli Lilly, Pfizer, Roche, and AstraZeneca outside the submitted work. A. Martínez-Marti reports personal fees and other support from Bristol Myers Squibb, F. Hoffmann-La Roche, Merck Sharp & Dohme, Pfizer, Boehringer Ingelheim, MSD Oncology, and AstraZeneca outside the submitted work. J. de Castro-Carpeño reports grants and personal fees from AstraZeneca, Bristol Myers Squibb, Merck Sharp & Dohme, and F. Hoffmann-La Roche, as well as personal fees from Boehringer Ingelheim, Amgen, Bayer, Lilly, Janssen-Cilag, Takeda, Novartis, and Pfizer outside the submitted work. R. Bernabé Caro reports other support from Bristol Myers Squibb and AstraZeneca, as well as grants from Roche outside the submitted work. S. Viteri reports personal fees from BMS, Puma, AstraZeneca, Reddy Pharma, Takeda, and Janssen, as well as personal fees and non-financial support from MSD, Merck, Roche, and OSE Immunotheraputics outside the submitted work. B. Massuti reports grants from Spanish Lung Cancer Group during the conduct of the study, as well as advisory board travel expenses from Bristol Myers Squibb. H. Kadara reports grants from Johnson & Johnson outside the submitted work. I.I. Wistuba reports grants and personal fees from Genentech/Roche, Bayer, Bristol Myers Squibb, AstraZeneca/Medimmune, Pfizer, HTG Molecular, Merck, Guardant Health, and Novartis; personal fees from GlaxoSmithKline, Oncocyte, MSD, and Daiichi Sankyo; and grants from Adaptive, 4D, Takeda, Karus, Adaptimmune, EMD Serono, Iovance, Johnson & Johnson, Amgen, and Akoya outside the submitted work. A. Romero reports personal fees from Boehringer Ingelheim outside the submitted work. V. Calvo reports personal fees from Roche, BMS, MSD, AstraZeneca, and Boehringer Ingelheim outside the submitted work. M. Provencio reports grants from BMS during the conduct of the study; M. Provencio also reports grants and non-financial support from Roche, as well as grants from AstraZeneca, Takeda, and MSD outside the submitted work. No disclosures were reported by the other authors.

Authors' Contributions

M. Casarrubios: Formal analysis, investigation, visualization, methodology, writing–original draft. **A. Cruz-Bermúdez:** Conceptualization, resources, data curation, formal analysis, supervision, funding acquisition, investigation, visualization, methodology, writing–original draft, project administration, writing–review and editing. **E. Nadal:** Resources, data curation, investigation, writing–review and editing. **A. Insa:** Resources, data curation, investigation, writing–review and editing. **M.R. García Campelo:** Resources, data curation, investigation, writing–review and editing. **M. Lázaro:** Resources, data curation, investigation, writing–review and editing.

M. Dómine: Resources, data curation, investigation, writing–review and editing.
M. Majem: Resources, data curation, investigation, writing–review and editing.
D. Rodríguez-Abreu: Resources, data curation, investigation, writing–review and editing.
A. Martínez-Marti: Resources, data curation, investigation, writing–review and editing. **J. de Castro-Carpeño:** Resources, data curation, investigation, writing–review and editing. **M. Cobo:** Resources, data curation, investigation, writing–review and editing. **G. López-Vivanco:** Resources, data curation, investigation, writing–review and editing. **E. Del Barco:** Resources, data curation, investigation, writing–review and editing. **R. Bernabé Caro:** Resources, data curation, investigation, writing–review and editing. **N. Viñolas:** Resources, data curation, investigation, writing–review and editing. **I. Barneto Aranda:** Resources, data curation, investigation, writing–review and editing. **S. Viteri:** Resources, data curation, investigation, project administration, writing–review and editing. **B. Massuti:** Resources, data curation, investigation, writing–review and editing. **M. Barquín:** Data curation, formal analysis, investigation, visualization, methodology, writing–review and editing. **R. Laza-Briviesca:** Data curation, investigation, methodology, writing–review and editing. **B. Sierra-Rodero:** Data curation, investigation, methodology, writing–review and editing. **E.R. Parra:** Investigation, writing–review and editing. **B. Sanchez-Espiridion:** Investigation, project administration, writing–review and editing. **P. Rocha:** Investigation, writing–review and editing. **H. Kadara:** Investigation, writing–review and editing. **I.I. Wistuba:** Resources, writing–review and editing. **A. Romero:** Data curation, investigation, writing–review and editing. **V. Calvo:** Resources, data curation, investigation, writing–review and editing. **M. Provencio:** Conceptualization, resources, data curation, supervision, funding acquisition, investigation, writing–original draft, project administration, writing–review and editing.

References

1. Provencio M, Nadal E, Insa A, García-Campelo MR, Casal-Rubio J, Dómine M, et al. Neoadjuvant chemotherapy and nivolumab in resectable non-small-cell lung cancer (NADIM): an open-label, multicentre, single-arm, phase 2 trial. Lancet Oncol 2020;21:1413–22.

2. Forde P, Spicer J, Lu S, Provencio M, Mitsudomi T, Awad M, et al. Abstract CT003 - Nivolumab (NIVO) + platinum-doublet chemotherapy (chemo) vs chemo as neoadjuvant treatment (tx) for resectable (IB-IIIA) non-small cell lung cancer (NSCLC) in the phase 3 CheckMate 816 trial. In: Proceedings of the Annual Meeting of the American Association for Cancer Research; 2021 Apr 10–15; Philadelphia (PA).

3. Rizvi H, Sanchez-Vega F, La K, Chatila W, Jonsson P, Halpenny D, et al. Molecular determinants of response to anti-programmed cell death (PD)-1 and anti-programmed death-ligand 1 (PD-L1) blockade in patients with non-small-cell lung cancer profiled with targeted next-generation sequencing. J Clin Oncol 2018;36:633–41.

4. Ready N, Hellmann MD, Awad MM, Otterson GA, Gutierrez M, Gainor JF, et al. First-line nivolumab plus ipilimumab in advanced non-small-cell lung cancer (CheckMate 568): Outcomes by programmed death ligand 1 and tumor mutational burden as biomarkers. J Clin Oncol 2019;37:992–1000.

5. Borghaei H, Hellmann MD, Paz-Ares LG, Ramalingam SS, Reck M, O'Byrne KJ, et al. Nivolumab (Nivo) + platinum-doublet chemotherapy (Chemo) vs chemo as first-line (1L) treatment (Tx) for advanced non-small cell lung cancer (NSCLC) with <1% tumor PD-L1 expression: Results from CheckMate 227. J Clin Oncol 2018;36:9001.

6. Borghaei H, Langer CJ, Paz-Ares L, Rodríguez-Abreu D, Halmos B, Garassino MC, et al. Pembrolizumab plus chemotherapy versus chemotherapy alone in patients with advanced non-small cell lung cancer without tumor PD-L1 expression: A pooled analysis of 3 randomized controlled trials. Cancer 2020;126:4867–77.

7. Garassino M, Rodriguez-Abreu D, Gadgeel S, Esteban E, Felip E, Speranza G, et al. OA04.06 evaluation of TMB in KEYNOTE-189: pembrolizumab plus chemotherapy vs placebo plus chemotherapy for nonsquamous NSCLC. J Thorac Oncol 2019;14:S216–7.

8. Voong KR, Feliciano J, Becker D, Levy B. Beyond PD-L1 testing-emerging biomarkers for immunotherapy in non-small cell lung cancer. Ann Transl Med 2017;5:376.

9. Li S, Zhang C, Pang G, Wang P. Emerging blood-based biomarkers for predicting response to checkpoint immunotherapy in non-small-cell lung cancer. Front Immunol 2020;11:1–11.

10. Robins HS, Campregher PV, Srivastava SK, Wacher A, Turtle CJ, Kahsai O, et al. Comprehensive assessment of T-cell receptor β-chain diversity in αβ T cells. Blood 2009;114:4099–107.

11. Kidman J, Principe N, Watson M, Lassmann T, Holt RA, Nowak AK, et al. Characteristics of TCR repertoire associated with successful immune checkpoint therapy responses. Front Immunol 2020;11:1–11.

12. Poran A, Scherer J, Bushway ME, Besada R, Balogh KN, Wanamaker A, et al. Combined TCR repertoire profiles and blood cell phenotypes predict melanoma patient response to personalized neoantigen therapy plus anti-PD-1. Cell Reports Med 2020;1:100141.

13. Cham J, Zhang L, Kwek S, Paciorek A, He T, Fong G, et al. Combination immunotherapy induces distinct T-cell repertoire responses when administered to patients with different malignancies. J Immunother Cancer 2020;8:1–10.

14. Cha E, Klinger M, Hou Y, Cummings C, Ribas A, Faham M, et al. Improved survival with T cell clonotype stability after anti-CTLA-4 treatment in cancer patients. Sci Transl Med 2014;6:238ra70.

15. Wu TD, Madireddi S, de Almeida PE, Banchereau R, Chen YJ, Chitre AS, et al. Peripheral T cell expansion predicts tumour infiltration and clinical response. Nature 2020;579:274–8.

16. Reuben A, Zhang J, Chiou S-H, Gittelman RM, Li J, Lee W-C, et al. Comprehensive T cell repertoire characterization of non-small cell lung cancer. Nat Commun 2020;11:603.

17. Anagnostou V, Forde PM, White JR, Niknafs N, Hruban C, Naidoo J, et al. Dynamics of tumor and immune responses during immune checkpoint blockade in non–small cell lung cancer. Cancer Res 2019;79:1214–25.

18. Han J, Duan J, Bai H, Wang Y, Wan R, Wang X, et al. TCR repertoire diversity of peripheral PD-1 + CD8 + T cells predicts clinical outcomes after immunotherapy in patients with non–small cell lung cancer. Cancer Immunol Res 2020;8:146–54.

19. Zhang J, Ji Z, Caushi JX, El Asmar M, Anagnostou V, Cottrell TR, et al. Compartmental analysis of T-cell clonal dynamics as a function of pathologic response to neoadjuvant PD-1 blockade in resectable non–small cell lung cancer. Clin Cancer Res 2020;26:1327–37.

20. Vroman H, Balzaretti G, Belderbos RA, Klarenbeek PL, Van Nimwegen M, Bezemer K, et al. T cell receptor repertoire characteristics both before and following immunotherapy correlate with clinical response in mesothelioma. J Immunother Cancer 2020;8:1–7.

21. Looney TJ, Topacio-Hall D, Lowman G, Conroy J, Morrison C, Oh D, et al. TCR convergence in individuals treated with immune checkpoint inhibition for cancer. Front Immunol 2020;10.

22. Parra ER, Uraoka N, Jiang M, Cook P, Gibbons D, Forget MA, et al. Validation of multiplex immunofluorescence panels using multispectral microscopy for immune-profiling of formalin-fixed and paraffin-embedded human tumor tissues. Sci Rep 2017;7:1–11.

23. Love MI, Huber W, Anders S. Moderated estimation of fold change and dispersion for RNA-seq data with DESeq2. Genome Biol 2014;15:550.

24. Steinbaugh MJ, Pantano L, Kirchner RD, Barrera V, Chapman BA, Piper ME, et al. BcbioRNAseq: R package for bcbio RNA-seq analysis [version 2; peer review: 1 approved, 1 approved with reservations]. F1000Research. F1000 Research 2018;7:1976.

25. Gudmundsdottir H, Wells AD, Turka LA. Dynamics and requirements of T cell clonal expansion in vivo at the single-cell level: effector function is linked to proliferative capacity. J Immunol 1999;162:5212–23.

26. Binnewies M, Roberts EW, Kersten K, Chan V, Fearon DF, Merad M, et al. Understanding the tumor immune microenvironment (TIME) for effective therapy. Nat Med 2018;24:541–50.

27. Goodman AM, Castro A, Pyke RM, Okamura R, Kato S, Riviere P, et al. MHC-I genotype and tumor mutational burden predict response to immunotherapy. Genome Med 2020;12:45.

28. Shim JH, Kim HS, Cha H, Kim S, Kim TM, Anagnostou V, et al. HLA-corrected tumor mutation burden and homologous recombination deficiency for the prediction of response to PD-(L)1 blockade in advanced non-small-cell lung cancer patients. Ann Oncol 2020;31: 902–11.

29. O'Donnell JS, Teng MWL, Smyth MJ. Cancer immunoediting and resistance to T cell-based immunotherapy. Nat Rev Clin Oncol 2019; 16:151–67.

30. Joshi K, de Massy MR, Ismail M, Reading JL, Uddin I, Woolston A, et al. Spatial heterogeneity of the T cell receptor repertoire reflects the mutational landscape in lung cancer. Nat Med 2019;25:1549–59.

31. Danilova L, Anagnostou V, Caushi JX, Sidhom J-W, Guo H, Chan HY, et al. The mutation-associated neoantigen functional expansion of specific T cells (MANAFEST) assay: a sensitive platform for monitoring antitumor immunity. Cancer Immunol Res 2018;6:888–99.